Edelweiss Applied Science and Technology
ISSN: 2576-8484
Vol. 9, No. 4, 1201-1216
2025
Publisher: Learning Gate
DOI: 10.55214/25768484.v9i4.6225

Examining the structural design of deep pile foundation bridge under different directions of water movement

Ahmed Saeed Hakim[1*]
[1]Engineering Faculty, Islamic Azad University, Kermanshah, Iran; ahmed.s.88@outlook.com (A.S.H.).

Abstract: The impact of water movement presented by currents and waves poses significant challenges to marine structures, particularly in the structural design of bridge structures. Pile foundation bridges, extending into the sea, are particularly susceptible to variations in the direction of these forces. This study investigates the structural response of such structures to directional changes in current-wave forces. A series of numerical simulations were performed using ABAQUS software to model the interaction of current and wave forces with varying directions. The study examined the dynamic response of bridge piers, specifically in terms of acceleration and displacement under multiple load conditions along the pile cap foundation. To validate the numerical results, previous experimental studies were considered. The findings show that the inherent frequencies of the bridge pier are increased when water is present. The greatest dynamic response was observed when the current-wave forces were longitudinal (90°), compared to other directional combinations (0°, 45°, 135°, and 180°). The influence of the directional disparity between current and wave forces is substantial and must not be overlooked in bridge design. Therefore, accounting for the interaction between current and wave direction is critical for the structural integrity of deep-water bridges.
Keywords: *ABAQUS software, Current-wave, Deepwater bridge, Directional effect, Pile foundation, Structural response.*

1. Introduction

To meet the requirements of construction and housing, there is a great need to exploit marine areas through the establishment of large cities that enable governments to accommodate the growing population [1]. To ensure easy traffic between these cities, there is a necessity to build sea-crossing bridges. The presence of these cities within marine areas exposes their bridges to the common water current and wave forces, which threaten the safety of these marine bridge structures [2, 3].

Deepwater coastal bridges frequently employ pile foundations because of how easily they can be built while still being stable [4, 5]. Pile foundation bridges mainly consist of a group of piles, an elevated pile cap, a pier, and a superstructure. The occurrence of this type of foundation in deepwater makes its piles and part of its pile cap exposed to sea forces, which contributes to the destabilization of the bridge pier [6]. On the other hand, because of the rarity of simultaneous severe current-wave events, industrial society in the world has not yet accepted the combination of precisely current and wave loads for design consideration [7]. However, data collected over the past 50 years in the world revealed that many powerful earthquakes had struck during the winter or spring, when the likelihood of experiencing moderate to severe water conditions was high [8].

Current literature about the structural response of such a pile foundation bridge under the combined action of wave is still of major interest to researchers in this field. Huang, et al. [9] modeled the behavior of coastal bridges exposed combined action of sea current and waves. To study the impact of sea wave-current action on the dynamic response of the pier and the distribution law of hydrodynamic forces along the altitude of the pier under various load conditions, Ding, et al. [10] developed a fifty

History: Received: 17 February 2025; Revised: 13 March 2025; Accepted: 17 March 2025; Published: 14 April 2025
* Correspondence: ahmed.s.88@outlook.com

reduced scale bridge pier model in accordance with the similarity principle. Cheng, et al. [11] simulated the wave, and current loads to investigate the dynamic analysis of a floating bridge finite element model using ABAQUS software. Liu, et al. [12] created a thirty-two reduced model of a pier-pile using steel wires and micro concrete to research how pier foundations behave in the presence of water and air. The experimental results indicated that the seismic response of the submerged bridge members is amplified because of the hydrodynamic pressure effect. Azadbakht and Yim [13] examined the hydrodynamic loads applied on bridge members which exposed to joint current and waves forces and finding the Mathematical formulation of inertia and drag forces coefficients. Hong, et al. [14] conducted experimental works to determine the transient performance of a large diameter pile under the combined current and wave activities. Niu, et al. [15] simulated the long-term performance of under scour and corrosion.

From the abovementioned theoretical and practical studies, several assumptions were made to address the challenging interplay between dynamic loads and models. Moreover, it lacks a study of the structural behavior of a bridge pier with a pile cap foundation wholly or partially immersed in water and under the combined influence of water current-wave actions. To simulate the actual situation and provide a clear view of this behavior of the bridge pier, which exposed its elevated pile-cap to the combined influence, an experimental test and numerical validation were used in this study.

The generation of sea currents in marine environments is the result of the movement of water particles which are controlled by the wind and density differences, while the generation of sea waves is caused by winds and radiates in all directions away from turbulence [16]. This means that waves do not always travel in the same direction as currents, i.e. waves and currents may travel in opposite directions [17-19]. The current-wave action may act in multiple directions due to the length of coastal bridges, which can reach tens of kilometers [20]. For bridges, the impact of waves and current flowing in the other direction is frequently more harmful.

This study first outlines the design of a pile foundation bridge. Second, the process of partially and totally pile-cap submerged in water and subjected to simultaneously test of current-wave with different directions, is introduced. Third, the peak accelerations and displacements of the pier are studied through the test data. Fourth, a three-dimensional numerical model is built, using the ABAQUS software and validated using previous experimental studies. Fifth, the validated model is used to find the effect of different directions of applied currents and waves. The results can be adopted as a reliable reference for further research and practical engineering.

2. Numerical Modelling

2.1. Model Design

This study aims to find structural behavior of a bridge with a pile foundation that was constructed in the common environment. As shown in Figure 1, the Songhua pile foundation bridge located in China Deng, et al. [20] was selected for the case study.

The selected foundation has nine piles with a height above scour line of 12m and a square cap of 12 m on each side. Also, there is a rectangular pier on top of the pile cap with dimensions of 3.0m x 4.8m. According to the selected case study, the main parts of the model are sketched in Figure 2 (a). The reinforced concrete material, as presented in see Figure 2 (b), was employed to produce the concrete model [21]. The influence of the bridge superstructure on the pier is performed in the form of a hummer as it is. The other elements of the superstructure with traffic loads are simplified as a concentrated mass on the top of the pier.

Figure 1.
Case study pile foundation bridge.

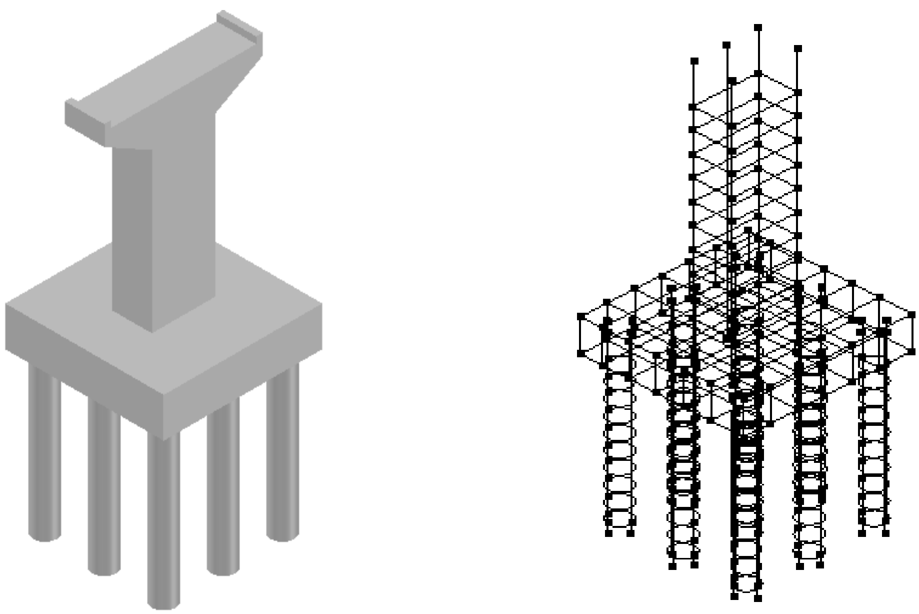

(a) Concrete partners. (b) Details of the reinforcement.

Figure 2.
Details of a typical FE case study model.

2.2. Force Cases

The physical circumstances of the appropriate issue must be well matched with the boundary conditions. Clamped Feet was chosen in order to investigate the loads that affected the software model under the assumption that the pile group is completely stable, like in the case study [21].

In the selected model, supplementary weight was used to represent the range of forces that bridges typically carried across their traffic loads and other live loads [22, 23]. The chosen load was dispersed

Edelweiss Applied Science and Technology
ISSN: 2576-8484
Vol. 9, No. 4: 1201-1216, 2025
DOI: 10.55214/25768484.v9i4.6225

throughout the top surface of the superstructure of the bridge as traffic load scenarios in order to compare the outcomes of the two models.

In Figure 3 (a), it can be noticed how currents and waves are projected as forces affecting the parts of the numerical model and in the desired direction. This program gives great ease and smoothness to the representation of these forces with the required characteristics. Mesh generation is conducted, as mentioned by Wei, et al. [24] to the proposed model with 0.001m with 12045–18750 Quadrated shape of element (Figure 3 b).

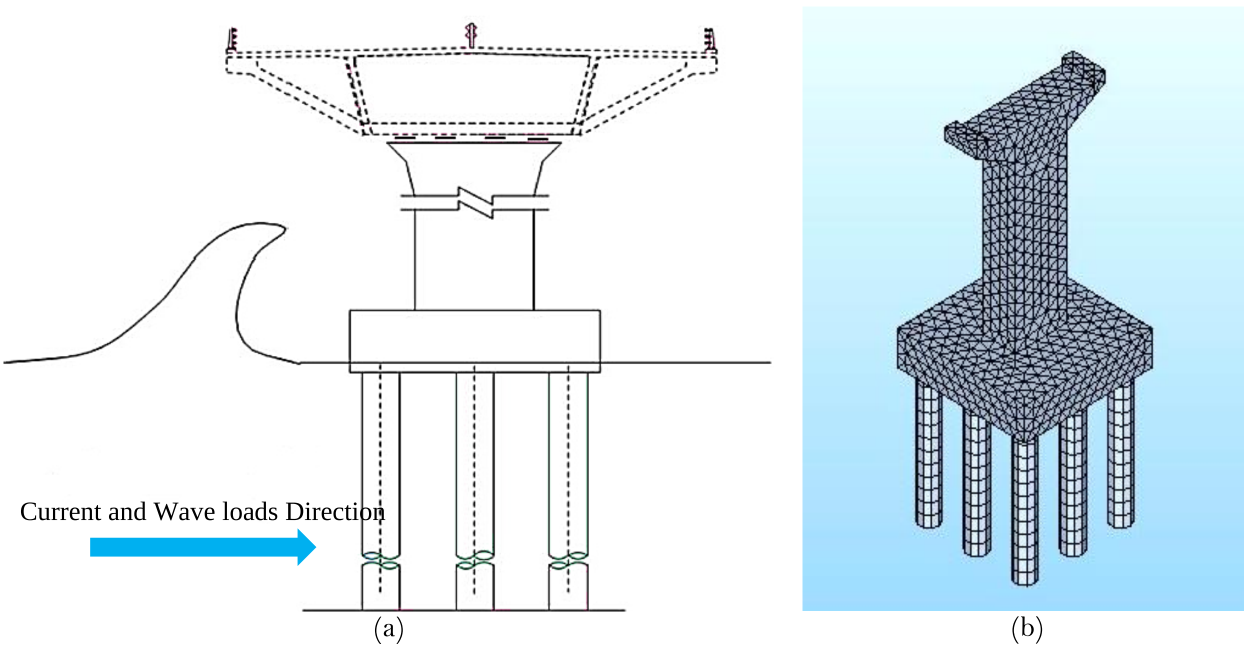

Figure 3.
Applied load cases.

2.3. Structural Design Equations

The structural design of deep pile foundation bridges under different water movement directions requires a combination of geotechnical, structural, and hydrodynamic calculations. This section presents the governing equations for pile capacity, concrete and reinforcement design, wave-current force interaction, dynamic response analysis, and stability checks.

The axial load-carrying capacity (Q_u) of a single pile is determined by considering both skin friction and end-bearing resistance [25]:

$$Q_u = Q_s + Q_p \tag{1}$$

where: Q_s = Shaft resistance (skin friction) and Q_p = End-bearing capacity

The shaft resistance is given by:

$$Q_s = \sum f_s A_s \tag{2}$$

where: f_s = Unit skin friction resistance and A_s = Surface area of the pile in contact with soil

The end-bearing capacity is given by:

$$O_p = q_p A_p \tag{3}$$

where: q_p= Unit end-bearing resistance and A_p = Cross-sectional area of the pile tip

For cohesive soils (clays):

$$q_p = N_c c \tag{4}$$

DOI: 10.55214/25768484.v9i4.6225

where: N_c = Bearing capacity factor (typically 9 for deep foundations) and c = Undrained shear strength of soil [26].
For cohesionless soils (sands and gravels):

$$q_p = 0.5\gamma' B N_q \quad (5)$$

where: γ'= Effective unit weight of soil, B = Pile base width and N_q= Bearing capacity factor (dependent on soil friction angle)
Lateral load capacity is evaluated using the elastic foundation beam equation:

$$EI\frac{d^4y}{dx^4} + ky = 0 \quad (6)$$

where: E = Elastic modulus of pile material, I = Moment of inertia of pile cross-section, y = Lateral displacement, and k = Soil subgrade modulus
For lateral deflection at the pile head:

$$y_{max} = \frac{HL^3}{3EI} \quad (7)$$

where: H = Applied lateral load and L = Embedded length of pile.
The ultimate moment capacity (M_u) of a reinforced concrete section is given by:

$$M_u = A_s f_y \left(d - \frac{a}{2}\right) \quad (8)$$

where: A_s = Area of tensile reinforcement, f_y = Yield strength of reinforcement, d = Effective depth of the section and a = Depth of the equivalent rectangular stress block, given by:

$$a = \frac{\beta_1 c}{\emptyset} \quad (9)$$

where: β_1 = Stress block coefficient (depends on concrete strength), c = Neutral axis depth and $\emptyset$ = Strength reduction factor
The nominal shear capacity (V_n) is given by:

$$V_n = V_c + V_s \quad (10)$$

where: V_c = Shear strength provided by concrete

$$V_c = 0.17\lambda\sqrt{f_c'}bd \quad (11)$$

V_s = Shear strength provided by shear reinforcement (stirrups)

$$V_s = \frac{A_v f_u d}{s} \quad (12)$$

where: A_v= Area of shear reinforcement per spacing and s = Spacing of stirrups.
The force exerted by water currents and waves on the pile foundation is evaluated using Morison's equation:

$$F = \frac{1}{2}C_D\rho A U^2 + C_M\rho A V\frac{dU}{dt} \quad (13)$$

where: C_D = Drag coefficient, C_M = Inertia coefficient, ρ = Water density, A = Projected area of the pile, U = Flow velocity, V = Volume of displaced fluid, and dU/dt = Acceleration of flow
The natural frequency of a bridge pier in the presence of water is estimated as:

$$f_n = \frac{1}{2\pi}\sqrt{\frac{k}{m_e}} \quad (14)$$

where: k = Equivalent stiffness of the pile foundation system and m_e = Effective mass of the bridge pier including added mass due to water
The efficiency of a pile group (E) in resisting loads is estimated using the Converse-Labarre equation:

$$E = 1 - (n-1) \times \alpha \quad (15)$$

where: n = Number of piles in the group and α = Efficiency factor (depends on pile spacing and soil conditions)
Scour depth (D_s) is estimated using empirical equations such as:

$$D_s = K_s \left(\frac{q}{V}\right)^n \quad (16)$$

where: K_s = Empirical coefficient, q = Flow discharge per unit width, V = Velocity of water flow and n = Empirical exponent
The critical scour depth should be compared with the pile embedment depth to ensure stability.

2.4. Model Calibration

To validate the similitude principles and model design employed in this work, the top displacement and peak acceleration of the model are compared with those of the prototype [27-29]. This calibration step was carried out using the finite element ABAQUS software, and the outcomes demonstrated that the model simulation process has an effective, with a well contract with the selected case study prototype and the test model .

The prototype and the entire model are compared to the first four major natural frequencies. Table 1 displays the results of the modal analysis. The dependability of the model design is demonstrated by the fact that there are minor inaccuracies between the prototype and the model, with the largest difference between the frequency value of the prototype and the model being less than 4%.

Table 1.
Verification of the prototype's and model's frequency similarity relationship.

Approach	Physics model (Hz)		Numerical model (Hz)	Maximum Error (%)
	f_p	f_p/S_f	f_m	
I.	0.84	3.75	3.65	2.71
II.	2.60	11.64	11.42	2.03
III.	3.86	17.27	16.61	4.18
IV.	6.55	29.31	28.82	1.75

2.5. Simulation Circumstances

According to data collected from studies, especially in the Asian region, wave intensity and period conditions with a recurrence time of 100 years were adopted. A wave theory with a wavelength of 2 meters and a period of 20 seconds was used. Furthermore, the current speed in the studied area is expected to be 2 meters/second [29]. Furthermore, it is anticipated that the current velocity in the examined region is 2 m/s [29]. In the trials, regular waves and uniform currents were employed, respectively. As test circumstances, a current speed of 0.2 meter/second and 0.02m as wave period, 0.1 m as wave length, and 2 m as wave depth. Wang, et al. [30] state that short waves and moderate current are typically regarded as typical current and wave conditions.

The water forces excitation can act in a longitudinal or transverse direction or in between bridge members [31, 32]. The fervor affected by these forces is supposed to move the bridge in five directions i.e. $\theta = 0^{\circ}, 45^{\circ}, 90^{\circ}, 135^{\circ} and\ 180^{\circ}$. The test used five different water heights (0.3, 0.35, 0.50, 0.60, and 0.80 m) to fully examine the combined impact of the wave and current on the pile foundation bridge pier's structural reaction. The previously specified test variables are included in Table 2.

Edelweiss Applied Science and Technology
ISSN: 2576-8484
Vol. 9, No. 4: 1201-1216, 2025
DOI: 10.55214/25768484.v9i4.6225

Table 2.
Present research test factors.

Water depth (m)		Current speed (m/sec)		Wave properties (m, m, sec)		Direction (°)	
H1	0.30	C	0.10	W	0.02, 0.1, 2	θ1	0°
H2	0.35					θ2	45°
H3	0.50					θ3	90°
H4	0.60					θ4	135°
H5	0.80					θ5	180°

Waves that do not follow the currents' paths can occur in the environments of big rivers, seas, and oceans due to certain natural factors [33, 34]. The behavior of the marine structures exposed to it becomes confused as a result of this occurrence [35, 36]. It was suggested to investigate the direction difference between current and wave at various angles, as illustrated in Figure 4 and tabulated in Table 3, since the numerical model developed for this study provides a state of ease and smoothness in shedding the effective forces in various directions, in addition to the earthquake directions [37].

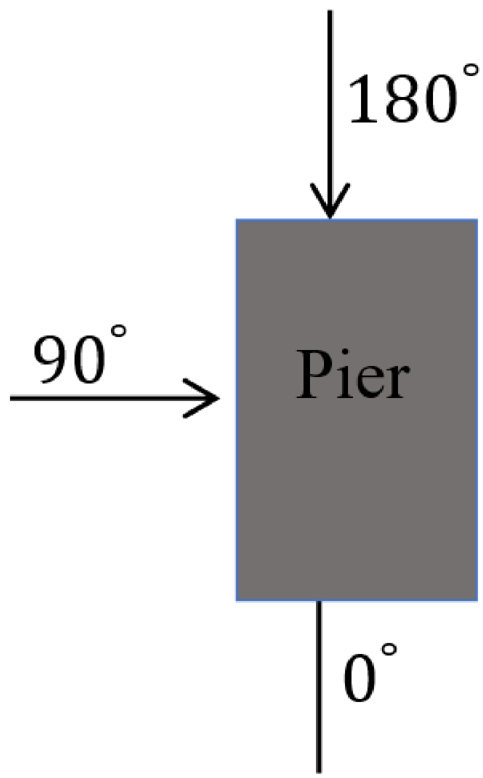

Figure 4.
Sketch to present impact loads directions.

Table 3.
Current-wave-earthquake direction states.

State	Current Dir.	Wave Dir.
1	0°	90°
2	0°	180°
3	90°	0°
4	180°	0°

Edelweiss Applied Science and Technology
ISSN: 2576-8484
Vol. 9, No. 4: 1201-1216, 2025
DOI: 10.55214/25768484.v9i4.6225

3. Results and Discussion

The joint current wave analysis of the bridge pier looks at the acceleration at the height of the pier and displacement of the top of the pier relative to the bottom to determine the structural response of the pier. The displacement of the pier top relative to the pier bottom is the most important factor in analyzing the deformation of the bridge pier. The absolute acceleration of the pier top under the impact of water loads is the most significant factor influencing deck motion. As shown in Figure (5), the acceleration and displacement along the body of the pier are computed.

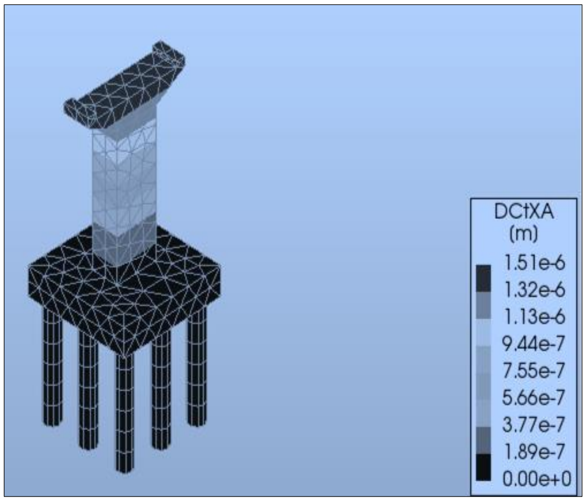

(a) Displacement response.

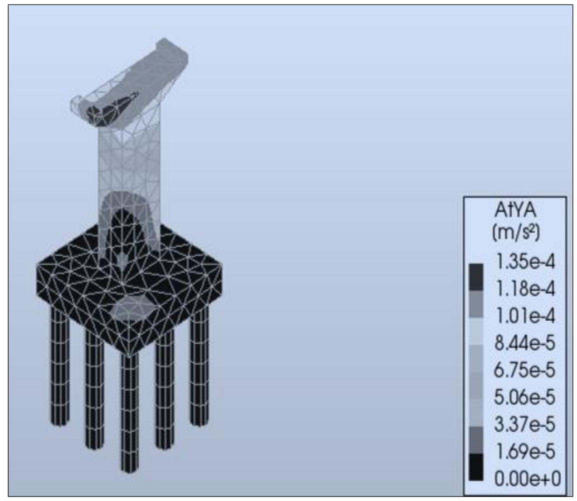

(b) Acceleration response.

Figure 5.
Displacement and acceleration responses of numerical models.

Figures (6 to 10) illustrated the studied five current-wave directions (0°, 45°, 90°, $135^{\circ}$and 180°). From Figures 6 to 10, it can be shown that the relative displacement increased and peaked at its highest point at the top of the pier. Also, it is worth noting that the greatest acceleration was found at the height of 0.6 m of the pier, and this may be because of the superstructure mass load of the pier. It can be also noticed that the water height of 0.675 m (H4) has the greatest effect in terms of acceleration and displacement, and the reason for it because the greater weight of the cap contrast to pile mass and the pier mass, then comes the other water depth H5, H3, H2, and H1, respectively.

The results approved that the effect of the combined actions of current and waves increases concerning direction impact in the transverse direction ($\theta 3$) and decreases as moves away from the transverse side, this is what makes the pier affected by its narrow side, which makes it affected more frequently than the wide side.

It was also found that when the direction with a transverse impact at an angle of 90° ($\theta 3$) on the bridges has the largest action in terms of displacement and acceleration. Its impact at the water height (H4) reached 6.8mm for displacement and 0.304g for acceleration, while the impact of the angles 45° ($\theta 2$) and 135°($\theta 5$) is approximately equal, with the approximate displacement of 6.075mm and approximately acceleration of 0.2625g, and they both turn less than ($\theta 3$) and greater than angles 0°($\theta 1$) and 180°($\theta 5$), which reached approximately 5.474mm and 0.2615g, for displacement and acceleration, respectively. Therefore, the direction of the effect of the impact force has a pivotal effect when studying the jointly current-wave actions. Table 4 lists the water heights and various circumstances (H1, H2, H3, and H5).

ISSN: 2576-8484
Vol. 9, No. 4: 1201-1216, 2025
DOI: 10.55214/25768484.v9i4.6225

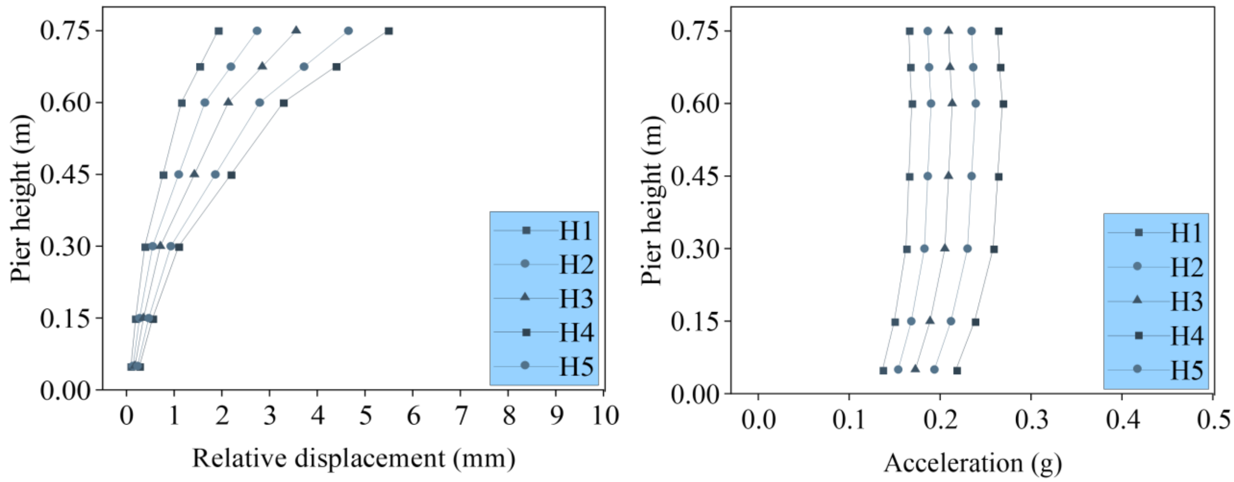

Figure 6.
Acceleration and Relative displacement under C-W- θ1.

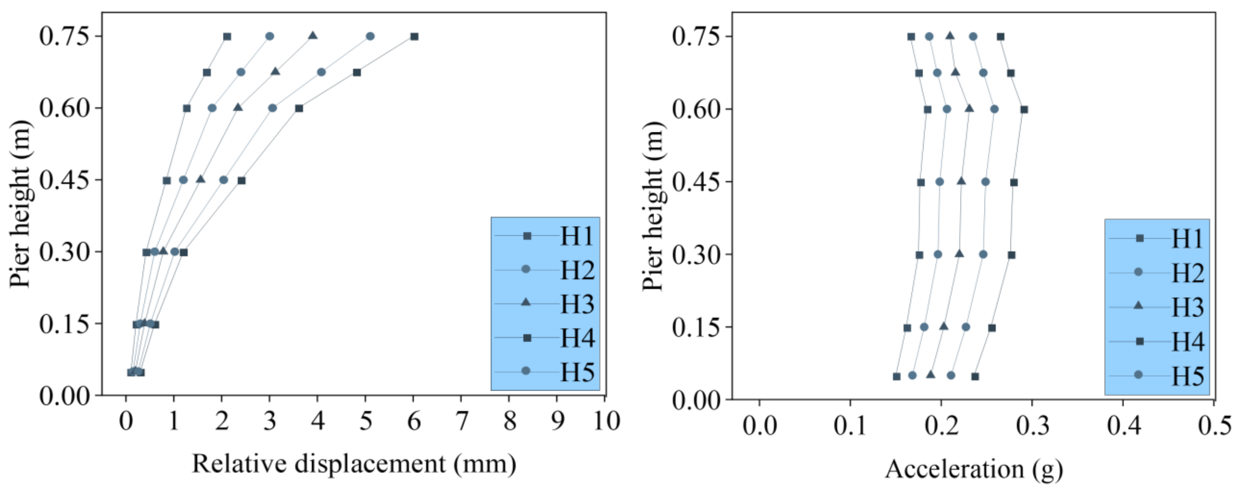

Figure 7.
Acceleration and Relative displacement under C-W- θ2.

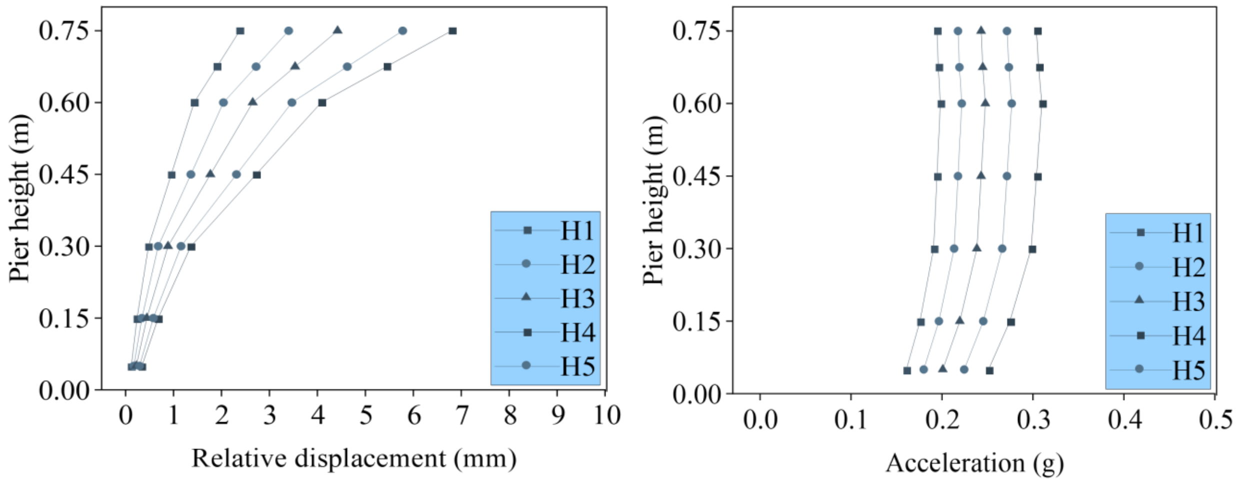

Figure 8.
Acceleration and Relative displacement under C-W- $\theta 3$.

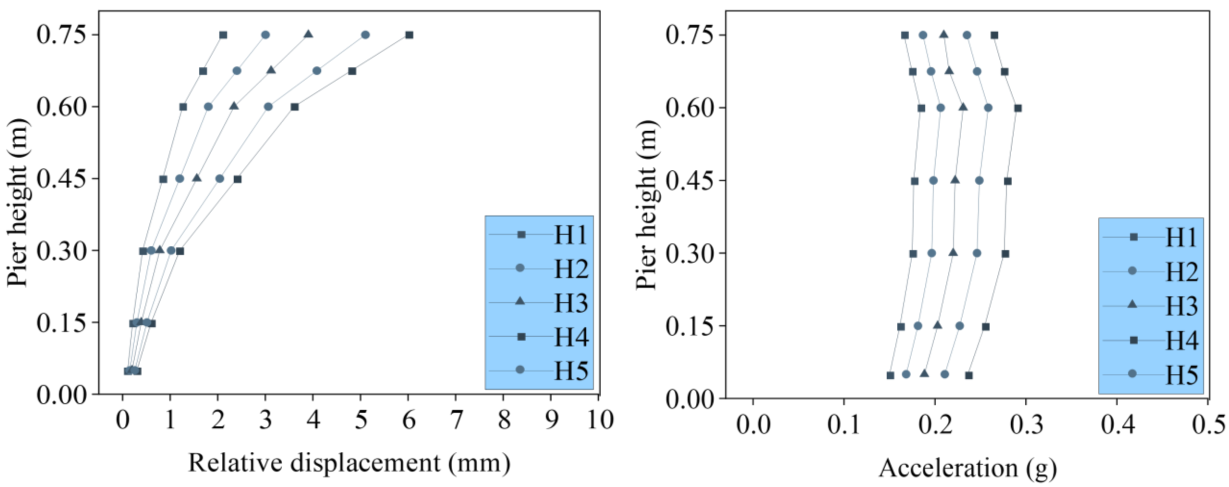

Figure 9.
Acceleration and Relative displacement under C-W- $\theta 4$.

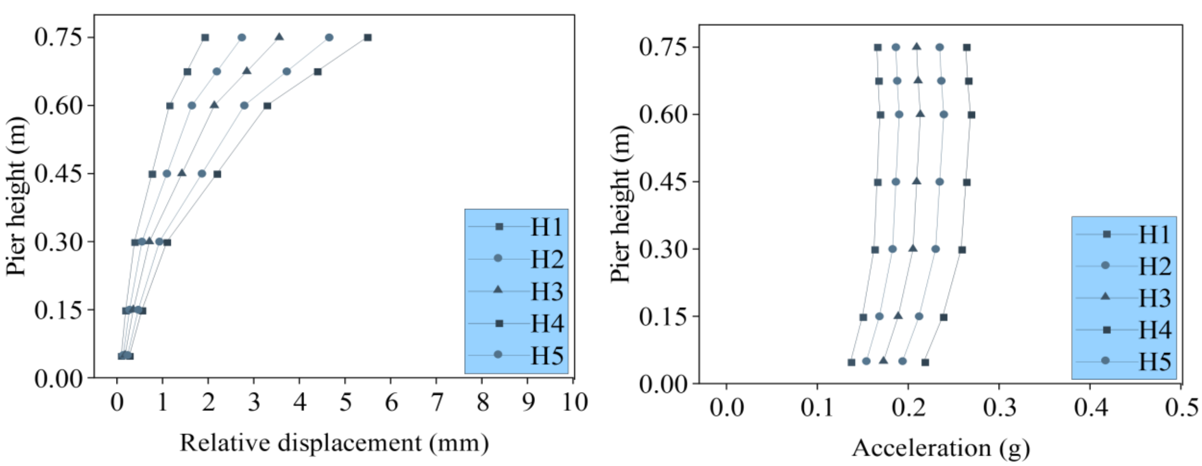

Figure 10.
Acceleration and Relative displacement under C-W- $\theta 5$.

Table 4.
Acceleration and Peak relative displacement under different conditions.

Load Type	H_1 = 0.3m		H_1 = 0.35m		H_1 = 0.5m		H_1 = 0.6m		H_1 = 0.8m	
	D.	A.	D.	A.	D.	A.	D.	A.	D.	A.
C-W- $\theta 1$	2.01	0.17	2.87	0.20	3.74	0.22	5.75	0.28	4.89	0.25
C-W- $\theta 2$	2.21	0.17	3.15	0.20	4.10	0.22	6.31	0.28	5.36	0.25
C-W- $\theta 3$	2.50	0.20	3.57	0.23	4.64	0.26	7.14	0.32	6.07	0.29
C-W- $\theta 4$	2.20	0.17	3.15	0.19	4.10	0.22	6.31	0.28	5.36	0.25
C-W- $\theta 5$	2.01	0.17	2.87	0.19	3.73	0.22	5.75	0.27	4.88	0.24

In order to apply the numerical model created for this study to tests that are not possible to conduct in a lab, a validation of the numerical model's output was done using the test model's output. The outcomes of the earlier experimental investigations carried out by Alsultani, et al. [18] provided evidence of this.

As seen in Figure 11 (a and b), the (C-W-E3) test carried out in ABAQUS was validated, and the results showed good agreement between the laboratory (Experimental) results (ER) and those performed through the software (Numerical results) (NR). All five laboratory and numerical tests underwent several statistical analyses, and the most recent one also revealed a high degree of acceptance in the results, with the peak coefficient value reaching 0.94 and the lower (R^2) non falling under 0.88, as shown in Table 5. Based on these findings, it can be said that the mathematical framework is capable of accurately representing the phenomena, with results typically reaching a semi-perfect match.

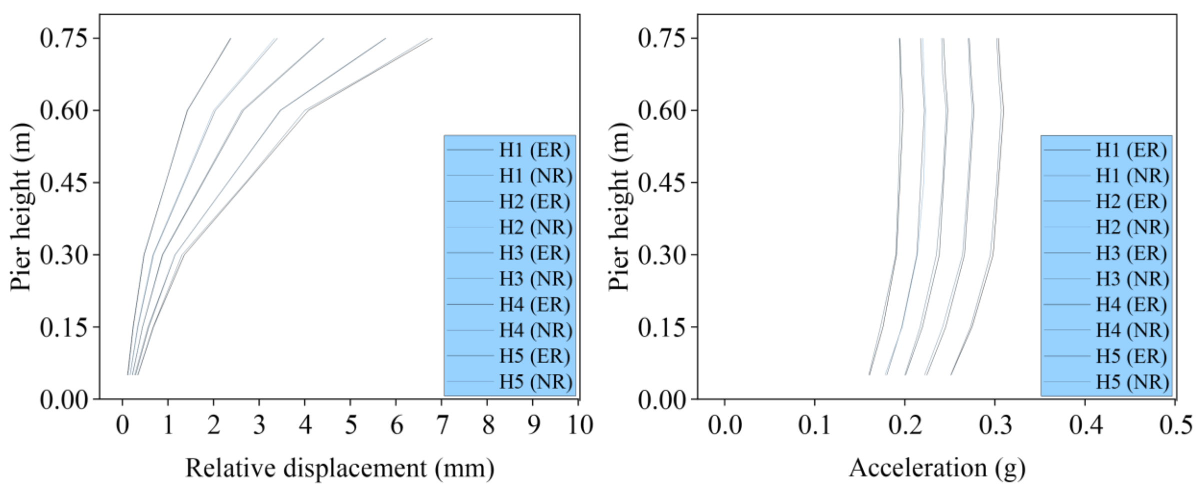

Figure 11.
Numerical results (NR) and Experimental results (ER) under C-W-E3.

Table 5.
Statistical comparison of numerical and experimental data using the R^2 indicator.

Test State	H_1 = 0.3m		H_1 = 0.35m		H_1 = 0.5m		H_1 = 0.6m		H_1 = 0.8m	
	D.	A.	D.	A.	D.	D.	A.	D.	A.	D.
C-W- $\theta 1$	0.90	0.93	0.93	0.93	0.92	0.91	0.92	0.92	0.91	0.92
C-W- $\theta 2$	0.94	0.94	0.94	0.94	0.93	0.93	0.93	0.93	0.93	0.93
C-W- $\theta 3$	0.94	0.93	0.93	0.93	0.93	0.93	0.93	0.93	0.93	0.93
C-W- $\theta 4$	0.92	0.93	0.88	0.92	0.91	0.94	0.93	0.92	0.92	0.93
C-W- $\theta 5$	0.93	0.94	0.92	0.93	0.94	0.91	0.94	0.93	0.91	0.94

From Figures (12 to 15), it can be seen in the multi-direction of applied forces and model analysis. The results show that the influence of the direction of the water currents and waves has an effect that cannot be ignored. It was found that when the wave and the current is 90°, the response of the pier increases by 20% from the normal condition ($0^{\circ}, 90^{\circ}$), which is indicated the Figure 12. The reason for this is that the pier was affected by these two convergent directions. But in the case of the wave being at an angle of 180 degrees, the response is reduced to -20%, which is shown in Figure 13. As for the change in the angle of the current relative to the wave, its effect does not exceed 10% with direction 90° (Figure 14) and -10% with 180°(Figure 15).

In Summary it can be noted that the largest pier response was found when the current and wave were in one direction (the angle between them is 0°), as the effect reached 30%. The results also showed that the least behavior, reaching -30%, which is when the current and wave are in one direction (the angle between them is 0°).

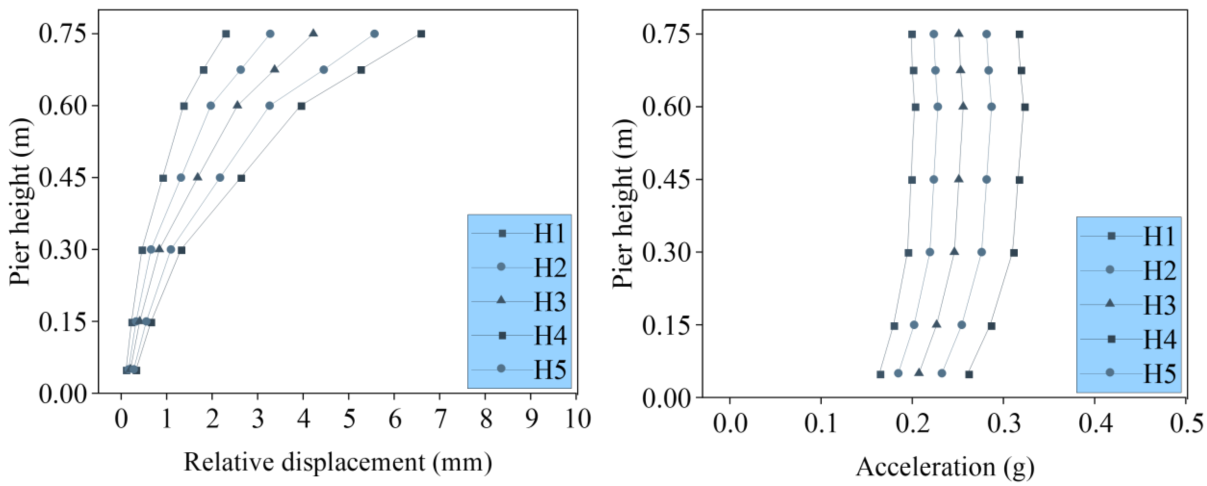

Figure 12.
Relative displacement and acceleration under state (1).

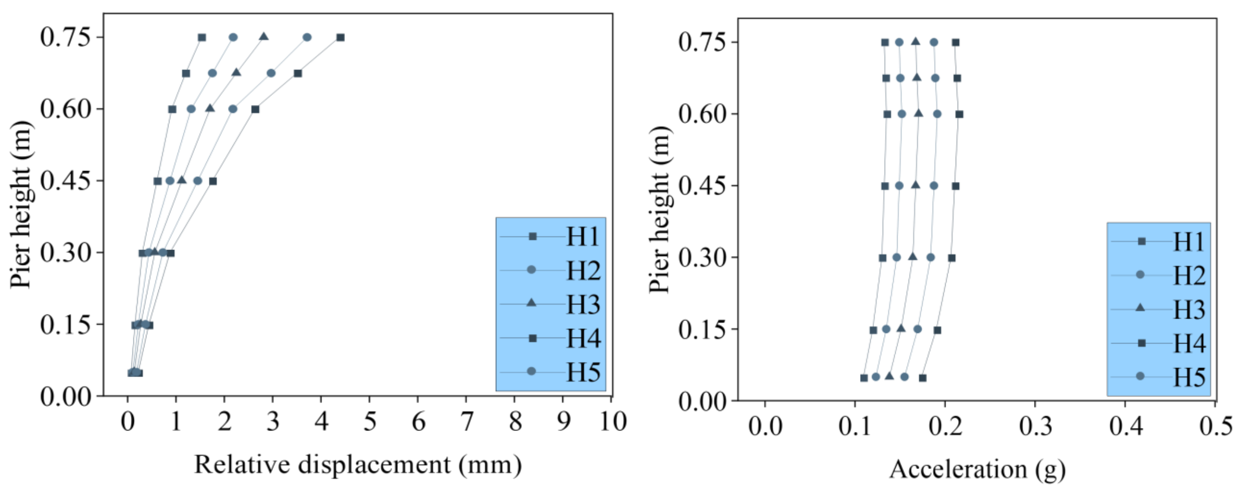

Figure 13.
Relative displacement and acceleration under state (2).

Edelweiss Applied Science and Technology
ISSN: 2576-8484
Vol. 9, No. 4: 1201-1216, 2025
DOI: 10.55214/25768484.v9i4.6225

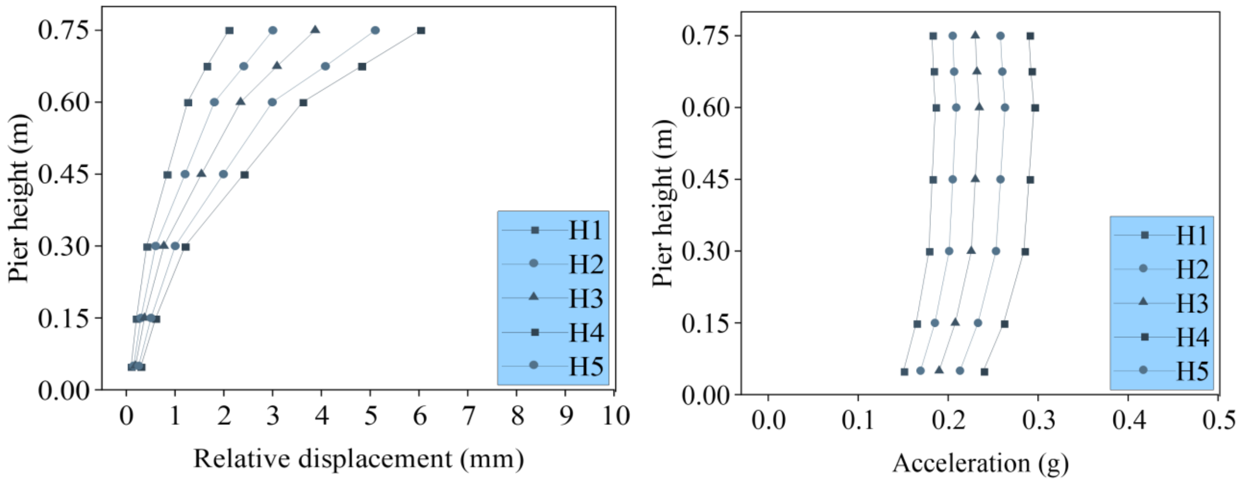

Figure 14.
Relative displacement and acceleration under state (3).

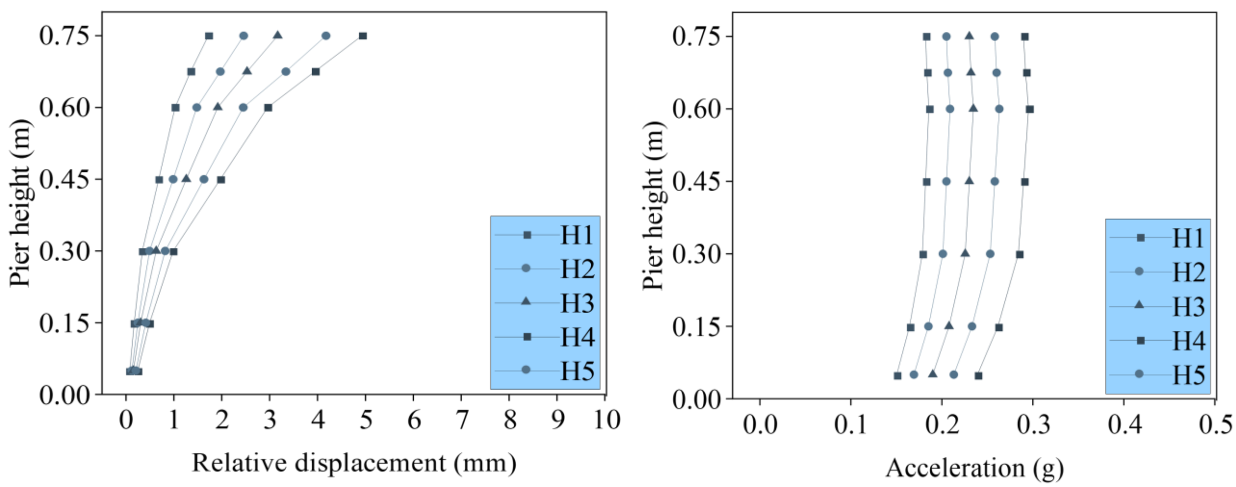

Figure 15.
Relative displacement and acceleration under state (4).

4. Conclusion

Under the combined current and wave impact directions, the behavior of the pile foundation pier for acceleration and relative displacement is altered in an obvious way. The conclusion outlines from this research can be numerated as follows:

(1) The relative displacement increased and reached its highest value at the top of the pier. Also, it is worth noting that the greatest acceleration was found at the height of 0.6 m of the pier, and this may be because of the superstructure mass load of the pier.

(2) The depth of the water rising into the pile cap has the greatest effect in terms of acceleration and displacement, and the reason for this is because the greater weight of the bridge cap of piles compared to pile and pier mass.

(3) The effect of the combined actions of current and waves increases concerning direction impact in the transverse direction and decreases as moves away from the transverse side, this is what makes the pier affected by its narrow side, which makes it affected more frequently than the wide side.

(4) The structural response of the pier concerning the change in path between current and wave does not exceed 10% with direction $90^{\circ}$and -10% with 180°.

Edelweiss Applied Science and Technology
ISSN: 2576-8484
Vol. 9, No. 4: 1201-1216, 2025
DOI: 10.55214/25768484.v9i4.6225

(5) When the wave at 90° direction relative to the current, the response of the pier increases by 20% and -20% for the direction 180° compared with the normal condition. Thus, the current-wave directionality cannot be ignored in the dynamic design of marine structures.
(6) High reaction of pier was found when the current and wave were in one direction (the angle between them is 0°) and at an angle of 90° relative to the direction of the earthquake, as the effect reached 30%.
(7) The results also showed that the least behavior, reaching -30%, which is when the current and wave are in one direction (the angle between them is 0°) and at an angle of 180° relative to the direction of the earthquake.
(8) The comparisons between numerical solutions and previous experimental results appeared with R^2 not less than 0.88, and this proved that ABAQUS model can be relied upon in performing other experiments that were not behaved in the laboratory system.

Transparency:

The author confirms that the manuscript is an honest, accurate, and transparent account of the study; that no vital features of the study have been omitted; and that any discrepancies from the study as planned have been explained. This study followed all ethical practices during writing.

Copyright:

References

[1] W. An-jie and Y. Wan-li, "Numerical study of pile group effect on the hydrodynamic force on a pile of sea-crossing bridges during earthquakes," *Ocean Engineering*, vol. 199, p. 106999, 2020. https://doi.org/10.1016/j.oceaneng.2020.106999
[2] E. Yu, S. Ren, H. Tang, Y. Li, and C. Fang, "Improvement on structural forms of pile group foundations of deepwater bridges," *Shock and Vibration*, vol. 2019, no. 1, p. 7381852, 2019. https://doi.org/10.1155/2019/7381852
[3] H. Wang, Q. Zhao, Q. Fang, Z. Chen, and A. Guo, "Comparative study on wave force calculation methods for bridge superstructures," *Structure and Infrastructure Engineering*, pp. 1-13, 2025. https://doi.org/10.1080/15732479.2025.2472368
[4] Z. X. Li, Q. Zheng, K. Wu, and Y. Shi, "Seismic analysis and test facilities of deep-water bridges considering water–structure interaction: a state-of-the-art review," *Earthquake Engineering and Resilience*, vol. 1, no. 1, pp. 21-39, 2022. https://doi.org/10.1002/eer2.8
[5] R. Alsultani, I. R. Karim, and S. I. Khassaf, "Experimental and numerical investigation into pile spacing effects on the dynamic response of coastal pile foundation bridges considering current-wave-earthquake forces," *Advances in Bridge Engineering*, vol. 6, no. 1, p. 1, 2025. https://doi.org/10.1186/s43251-024-00147-z
[6] Z. Cheng, S. Cong, and Z. Cheng, "Recent advances in composite caisson–pile foundation," *Marine Georesources & Geotechnology*, pp. 1-14, 2025. https://doi.org/10.1080/1064119X.2025.2468851
[7] J. Han, L. Pan, B. Lu, Z. Zhang, X. Bi, and B. Zhu, "Dynamic analysis of the wind-wave-current-bridge system considering pile-soil interaction," *Advances in Structural Engineering*, vol. 25, no. 15, pp. 3031-3043, 2022. https://doi.org/10.1177/13694332221114067
[8] R. Alsultani *et al.*, "The impact of climate change on the reinforcement durability of concrete bridge structures," *Open Civ Eng J*, vol. 18, p. e18741495337012, 2024. http://dx.doi.org/10.2174/0118741495337012240812105905
[9] B. Huang, B. Zhu, S. Cui, L. Duan, and Z. Cai, "Influence of current velocity on wave-current forces on coastal bridge decks with box girders," *Journal of Bridge Engineering*, vol. 23, no. 12, p. 04018092, 2018. https://doi.org/10.1061/(ASCE)BE.1943-5592.0001309
[10] Y. Ding, R. Ma, Y.-D. Shi, and Z.-X. Li, "Underwater shaking table tests on bridge pier under combined earthquake and wave-current action," *Marine Structures*, vol. 58, pp. 301-320, 2018. https://doi.org/10.1016/j.marstruc.2017.12.004
[11] Z. Cheng, Z. Gao, and T. Moan, "Numerical modeling and dynamic analysis of a floating bridge subjected to wind, wave, and current loads," *Journal of Offshore Mechanics and Arctic Engineering*, vol. 141, no. 1, p. 011601, 2019. https://doi.org/10.1115/1.4040561

[12] T. Liu, Z. He, and Y. Yang, "Vertical earthquake vulnerability of long-span spherical lattice shells with low rise-span ratios," *Engineering Structures*, vol. 207, p. 110181, 2020. https://doi.org/10.1016/j.engstruct.2020.110181

[13] M. Azadbakht and S. C. Yim, "Effect of trapped air on wave forces on coastal bridge superstructures," *Journal of Ocean Engineering and Marine Energy*, vol. 2, pp. 139-158, 2016. https://doi.org/10.1007/s40722-016-0043-9

[14] C. Hong, Z. Lyu, F. Wang, Z. Zhao, and L. Wang, "Wave-Current Loads on a Super-Large-Diameter Pile in Deep Water: An Experimental Study," *Applied Sciences*, vol. 13, no. 15, p. 8859, 2023. http://dx.doi.org/10.3390/app13158859

[15] S. Niu, Z. Liu, T. Guo, A. Guo, and S. Xu, "Modeling and Investigation of Long-Term Performance of High-Rise Pile Cap Structures Under Scour and Corrosion," *Journal of Marine Science and Engineering*, vol. 13, no. 3, p. 450, 2025. https://doi.org/10.3390/jmse13030450

[16] Y. Li, Z. Xu, and X. Lv, "The generation and propagation of wind-and tide-induced near-inertial waves in the ocean," *Journal of Marine Science and Engineering*, vol. 12, no. 9, p. 1565, 2024. https://doi.org/10.3390/jmse12091565

[17] Y. Chen, Y. Lv, K. Wu, and X. Huang, "Centrifuge shaking table study on the hydrodynamic effects on a pile foundation bridge pier in soft soil under earthquakes," *Marine Structures*, vol. 85, p. 103261, 2022. https://doi.org/10.1016/j.marstruc.2022.103261

[18] R. Alsultani, I. R. Karim, and S. I. Khassaf, "Dynamic response analysis of coastal piled bridge pier subjected to current, wave and earthquake actions with different structure orientations," *International Journal of Concrete Structures and Materials*, vol. 17, no. 1, p. 9, 2023. http://dx.doi.org/10.1186/s40069-022-00561-5

[19] E. Zhao, X. Xia, J. Gao, F. Jiang, X. Chen, and R. Liu, "Performance of coastal circular bridge pier under joint action of solitary wave and sea current," *Ocean Engineering*, vol. 250, p. 111033, 2022. https://doi.org/10.1016/j.oceaneng.2022.111033

[20] Y. Deng, Q. Guo, and L. Xu, "Experimental and Numerical Study on Modal Dynamic Response of Water-Surrounded Slender Bridge Pier with Pile Foundation," *Shock and Vibration*, vol. 2017, no. 1, p. 4769637, 2017. https://doi.org/10.1155/2017/4769637

[21] J. Zhang, K. Wei, Y. Pang, M. Zhang, and S. Qin, "Numerical investigation into hydrodynamic effects on the seismic response of complex hollow bridge pier submerged in reservoir: case study," *Journal of Bridge Engineering*, vol. 24, no. 2, p. 05018016, 2019.

[22] Z. H. Joudah *et al.*, "Effects of waste glass bottle nanoparticles and high volume of waste ceramic tiles on concrete performance when exposed to elevated temperatures: Experimental and theoretical evaluations," *Fire*, vol. 7, no. 12, p. 426, 2024. https://doi.org/10.3390/fire7120426

[23] R. F. Hasan, M. Seyedi, and R. Alsultani, "Assessment of haditha dam surface area and catchment volume and its capacity to mitigate flood risks for sustainable development," *Mathematical Modelling of Engineering Problems*, vol. 11, no. 7, 2024. https://doi.org/10.18280/mmep.110728

[24] K. Wei, J. Zhang, and S. Qin, "Experimental and numerical assessment into frequency domain dynamic response of deep water rigid-frame bridge," *Journal of Earthquake Engineering*, vol. 26, no. 1, pp. 307-330, 2022.

[25] T. J. Alfatlawi, N. J. Mansori, and R. A. Alsultani, "Stability assessment of Diaphram cellular cofferdams subjected to severe hydro-structural conditions," *The Open Civil Engineering Journal*, vol. 14, no. 1, 2020. https://doi.org/10.2174/1874149502014010044

[26] K. Wei, C. Zhou, M. Zhang, Z. Ti, and S. Qin, "Review of the hydrodynamic challenges in the design of elevated pile cap foundations for sea-crossing bridges," *Advances in Bridge Engineering*, vol. 1, pp. 1-30, 2020.

[27] F. Liang, X. Liang, and C. Wang, "Simplified added-mass model for evaluating the response of rectangular hollow bridge piers under earthquakes," *Journal of Bridge Engineering*, vol. 26, no. 10, p. 04021076, 2021.

[28] N. N. Mageed, R. Alsultani, and A. W. N. Abbas, "The Impact of Using Advanced Technologies in Sustainable Design to Enhance Usability and Achieve Optimal Architectural Design," *International Journal of Sustainable Development & Planning*, vol. 19, no. 11, 2024. https://doi.org/10.18280/ijsdp.191116

[29] L. Gao, Z. Liu, F. Dai, and J. Chen, "Response analysis of a long-span cable-stayed bridge with ultra-high piles subjected to near-fault ground motions considering deep-water, sedimentation, local site, and wave-passage effect," *Advances in Bridge Engineering*, vol. 5, no. 1, p. 34, 2024. https://doi.org/10.1186/s43251-024-00142-4

[30] P. Wang, M. Zhao, X. Du, J. Liu, and J. Chen, "Simplified evaluation of earthquake-induced hydrodynamic pressure on circular tapered cylinders surrounded by water," *Ocean Engineering*, vol. 164, pp. 105-113, 2018.

[31] Q. A. Saber *et al.*, "Structural finite element analysis of bridge piers with consideration of hydrodynamic forces and earthquake effects for a sustainable approach," *Mathematical Modelling of Engineering Problems*, vol. 12, no. 3, pp. 1071-1080, 2025. https://doi.org/10.18280/mmep.120334

[32] H. Jiang, B. Wang, X. Bai, C. Zeng, and H. Zhang, "Simplified expression of hydrodynamic pressure on deepwater cylindrical bridge piers during earthquakes," *Journal of Bridge Engineering*, vol. 22, no. 6, p. 04017014, 2017.

[33] H. A. Afan *et al.*, "Data-driven water quality prediction for wastewater treatment plants," *Heliyon*, vol. 10, no. 18, 2024. https://doi.org/10.1016/j.heliyon.2024.e36940

[34] R. Kouhdasti and N. Bouaanani, "An efficient procedure for modal seismic response analysis of axisymmetric structures surrounded by water," *Ocean Engineering*, vol. 304, p. 117771, 2024.

[35] E. Q. Shehab and R. Alsultani, "A new approach to sustainable environmental assessment for wastewater treatment plants-A case study in the central region of Iraq," *Ecological Engineering & Environmental Technology*, vol. 26, no. 1, 2025. https://doi.org/10.12912/27197050/194126

[36] J. Wang, Q. Ma, Z. Yang, J. Gao, and G. Wu, "Two types of wave-current interactions and their effects on extreme waves in directional seas," *Ocean Engineering*, vol. 266, p. 112637, 2022. https://doi.org/10.1016/j.oceaneng.2022.112637

[37] W. Hernandez, A. Viviescas, and C. A. Riveros-Jerez, "Water–structure interaction analysis of a segmental bridge using ambient vibration testing at different water levels," *Journal of Civil Structural Health Monitoring*, vol. 13, no. 8, pp. 1483-1497, 2023.